Interference Benefits of a Vector Delay Lock Loop (VDLL) GPS Receiver

Don Benson, *MITRE Corporation*

BIOGRAPHY

Don Benson received a B.S. in Physics and a M.S. in Aeronautics and Astronautics both from MIT. His previous work experience for AC Electronics, TASC, and Dynamics Research Corporation (DRC) involved design and evaluation of inertial instruments, inertial navigation systems, Kalman filters, gravity gradiometers, and GPS. Currently with the MITRE Corporation, he helps resolve interference and spectrum issues related to GPS; develops and evaluates new navigation concepts. Don has nineteen publications in the open literature resulting from his work activities and two patents.

ABSTRACT

The interference benefits of a vector delay lock loop (VDLL) GPS receiver are compared by simulation over those of a conventional receiver as a first step before hardware implementation. Besides improvement to interference performance, other benefits to the user include: no additional hardware, no increase in power requirements, no increase in weight, and no decrease in reliability. In addition simulation results show a VDLL receiver can implement different filter bandwidths to accommodate differences that may be expected in vertical and horizontal motions. A conventional receiver can not do this. VDLL can be implemented as part of an ultra-tightly coupled or a deeply integrated GPS receiver so that if the inertial system degrades or fails, the receiver has the interference benefits of VDLL.

INTRODUCTION

MITRE became involved with vector delay lock loop (VDLL) tracking when the use of a high power satellite was proposed as a GPS acquisition aid [1]. We reasoned that the high power satellite could also be used to enhance the ability to track in a higher interference environment if the power of the single space vehicle (SV) could be distributed over the tracking loops of the other satellites. This can be done since the loops can be coupled through the navigation solution if the receiver has VDLL implemented. The coupling of the tracking loops through the navigation solution was suggested by Spilker [2]. MITRE's work is extended to quantify the interference benefits of a VDLL GPS receiver. Clearly the receiver requires no additional hardware and, as a result, no increase in power, weight and size, and no decrease in reliability, all benefits to the general user as well as to the warfighter.

The preliminary results shown in this paper quantify the interference benefit. Also shown is a not so obvious result that the tracking loops can have different bandwidths for tracking horizontal and vertical motion. A conventional receiver cannot do this since in a conventional receiver each loop must track the user-to-satellite range motion. In addition to the numerical results, a different but equivalent way to derive VDLL equations than shown in Spilker [2] is discussed.

Finally, this paper compares interference performance equations for three types of GPS receivers, a VDLL receiver, an ultratight (UTC) or deep integration (DI) receiver, and VDLL embedded in a UTC or deep integration receiver. In the last type of receiver the interference performance can approach that of a VDLL receiver if the inertial components degrade.

1. ASSUMPTIONS AND DEVELOPMENT OF VDLL EQUATIONS

To more easily determine the interference benefit of a VDLL GPS receiver, we will assume that the carrier tracking loops lose lock first and then the receiver revert s to code tracking. That is, the receiver is no longer in what is called State 5 (code/carrier track), but the receiver is tracking the code (State 3). We can show that this is a reasonable assumption based on Table 3.3-4 from the GPS Receiver Application Module (GRAM) specification [3]. This table shows that the J/S ratios for State 5 are less than the J/S ratios for State 3; however, the accuracy for State 5 is better than that for State 3. We plan to verify this assumption in a latter effort and report.

Table 1. Unaided and Aided Tracking Requirements from Table 3.3-4 of GRAM Specification

Tracking State	J/S (dB) Unaided	J/S Aided	Pseudorange Accuracy (Meters, RMS)		Deltarange Accuracy (Wavelengths, RMS)	
			P(Y) Code	C/A Code	P(Y) Code	C/A Code
State 3 (Code Lock)	44 (C/A) 62 (P(Y))	44 (C/A) 62 (PY)) 65 (P(Y))	3.0	10.0	N/A	N/A
State 4 (Carrier Lock	31 (C/A) 41 (P(Y))	31 (C/A) 41 (P(Y))	3.0	10.0	0.5	0.5
State 5 (Code/Carrier Track)	31 (C/A) 41 (P(Y))	31 (C/A) 41 (P(Y))	1.0	5.0	0.1	0.1

The basic theme used in this paper is to determine the measurement equations and then characterize the measurement errors. Once this is done then the filter design to estimate the variables, such as code tracking errors, becomes relatively easy.

The pseudorange measurement is determined from the time difference between the time the code is received by the receiver (measured by the receiver clock) and the time that it was sent by the SV as time stamped by the satellite time. The pseudorange is then the time difference multiplied by ***c*** – the free space speed of electromagnetic propagation. However, because of the group delay when the signal passes through the medium that includes troposphere and ionosphere, the multiplier should not be ***c*** but something less. For now we will neglect the transmission effect and discuss this in a follow-on report. The code used for signal correlation is a replica code. The replica code is offset from the true code by the time delay as measured by the code tracking loop (the output of the discriminator). We will also assume an early power minus late power discriminator noting that other discriminators can be used.

Since we want to determine the improvement in interference performance of a VDLL over a conventional receiver, we need to determine measurement equations for both a conventional GPS receiver and a VDLL GPS receiver.

1.1 CONVENTIONAL RECEIVER MEASUREMENT EQUATIONS

For a conventional receiver we have the following equations for each SV being tracked:

$Z_{(EP-LP)1} = 2P_1\Delta T_{TL1} + \eta_{TL1}$ Discriminator measurement (1)

$\Delta Z_{PR1} = \Delta R_{m1} + c\Delta t_R + c\Delta T_{TL1}$ Pseudorange measurement (2)

$\Delta\dot{R}_{mm1} = F_R\Delta R_{mm1} + \eta_R$ Range motion model (3)

$\Delta\dot{t}_{Rm} = F_C\Delta t_{Rm} + \eta_C$ Receiver clock model (4)

$\Delta R_{m1} = HC_1\Delta R_{mm1}$ Range error from range motion model (5)

$\Delta t_R = HC_2\Delta t_{Rm}$ Time error from receiver clock model (6)

P_1 is the power at the input to the discriminator from SV_1. This power is the result of attenuation by receiver implementation losses, Doppler errors due to clock frequency drift and changes in line-of-sight velocity because we have assumed that we are no longer able to track the carrier plus Doppler frequency. The discriminator we have analyzed assumes an early minus late difference of one chip [4, pg. 348]. Other terms are defined below.

η_{TL1} is the interference or noise to the discriminator.

ΔT_{TL1} is the time offset between the true code and the replica code.

ΔR_{mm1} is a state space range motion model of dimension; *nm*. The range motion model and the receiver clock model when combined with the discriminator noise model basically determine the filter bandwidth. The pseudorange measurement is usually determined with respect to a nominal location and the range motion is with respect to the nominal.

ΔR_{m1} is the range error

F_R is the $nm \times nm$ matrix describing the range motion.

η_R is noise driving the range motion model.

F_R is the $nc \times nc$ matrix describing the receiver clock drift.

η_C is noise driving the receiver clock model.

Δt_{Rm} is a state space receiver clock model of dimension, *nc*.

HC_1 selects the range state from the range motion model. HC_2 selects the receiver time error state from the receiver clock model.

$$\Delta\rho_{m1} \equiv \Delta R_{m1} + c\Delta t_R \text{ is true pseudorange.} \quad (7)$$

In a conventional receiver the pseudorange measurements from each SV are inputs to the navigation calculation where position and receiver clock bias are estimated [5,pg.325]. The tracking errors, $c\Delta T_{TL1}$, are treated as pseudorange measurement noise in the navigation calculations of a conventional receiver.

1.2 VDLL RECEIVER MEASUREMENT EQUATIONS

An easy way to obtain equations for a VDLL receiver is simply to replace the range variable in the pseudorange measurement by its definition in terms of the navigation states as follows. If we know the satellite position we can express the range error, ΔR_{m1}, in terms of the user δx, δy, δz position errors as:

$$\Delta\rho_{m1} = \Delta R_{m1} + c\Delta t_R = \begin{bmatrix} \alpha_{x1} & \alpha_{y1} & \alpha_{z1} & 1 \end{bmatrix} \begin{bmatrix} \delta x \\ \delta y \\ \delta z \\ c\Delta t_R \end{bmatrix} \quad (8)$$

Where the α are the direction cosines from the x, y, and z axes to the range vector that points from the user to the satellite. That is, the range error for each satellite is the projection of the errors from the x, y, and z axes on each range direction. Thus for *n* SVs, we have *n* pseudorange measurements and *n* discriminator measurements:

$$Z_{(EP-LP)1} = 2P_1\Delta T_{TL1} + \eta_{TL1}$$
$$\vdots \qquad \text{Discriminator}$$
$$Z_{(EP-LP)n} = 2P_n\Delta T_{TLn} + \eta_{TLn}$$

measurements (*n* SVs) (9)

$$\begin{bmatrix} \Delta Z_{PR1} \\ \vdots \\ \Delta Z_{PRn} \end{bmatrix} = \begin{bmatrix} \alpha_{x1} & \alpha_{y1} & \alpha_{z1} & 1 \\ \vdots & \vdots & \vdots & \vdots \\ \alpha_{xn} & \alpha_{yn} & \alpha_{zn} & 1 \end{bmatrix} \begin{bmatrix} \delta x \\ \delta y \\ \delta z \\ c\Delta t_R \end{bmatrix} + c \begin{bmatrix} \Delta T_{TL1} \\ \vdots \\ \Delta T_{TLn} \end{bmatrix}$$

Pseudorange measurements (10)

Instead of having a range motion model as in a conventional receiver, now we can have separate motion models for all three axes as follows:

$$\delta\ddot{x}_m = F_x\delta x_m + w_{xm} \quad \text{x motion model} \quad (11)$$

$$\delta\ddot{y}_m = F_y\delta y_m + w_{ym} \quad \text{y motion model} \quad (12)$$

$$\delta\ddot{z}_m = F_z\delta z_m + w_{zm} \quad \text{z motion model} \quad (13)$$

$$\delta x = H_{xm}\delta x_m \quad \text{x position from x motion model} \quad (14)$$

$$\delta y = H_{ym}\delta y_m \quad \text{y position from y motion model} \quad (15)$$

$$\delta z = H_{zm}\delta z_m \quad \text{z position from z motion model} \quad (16)$$

$$\Delta\dot{t}_{Rm} = F_C\Delta t_{Rm} + \eta_C \quad \text{receiver clock model} \quad (17)$$

$$\Delta t_R = HC_2\Delta t_{Rm} \quad \text{time error from receiver clock model} \quad (18)$$

Usually there would be no distinction between the horizontal x and y motion statistics or bandwidth, but there can be a distinction between horizontal motion bandwidth and vertical motion bandwidth. As can be seen by comparing Equations (9-18) with Equations (1-6), the different bandwidth structure can be accomplished with a VDLL receiver but not a conventional receiver.

We also note from the equations for VDLL that the performance of VDLL depends upon the number of SVs in view and their geometry as determined by the direction cosines (α). The tracking performance of a conventional receiver does not depend upon these parameters.

2. ASSESSING INTERFERENCE PERFORMANCE

The procedure used to determine interference performance first models the tracking performance of a conventional receiver. The wideband noise floor represented by the noise term, η_{TL1}, is increased until the 1σ error of the tracking loop reaches 1/6 of a chip and the loop is then said to lose lock. The noise level when this occurs is noted. Now the procedure is applied to a VDLL receiver. In a VDLL receiver, the tracking loops are coupled through the navigation equations and all the tracking loops must be examined for loss of lock. The noise is increased until one of the tracking loops 1σ errors reaches 1/6 of a chip, then the measurements from that loop are not valid and not used. When that measurement is eliminated the 1σ errors of all the other tracking loops increase and the 1σ values are again examined. If none of the 1σ errors exceed 1/6 of a chip, there is still interference margin left and the noise is increased until another loop loses lock and is eliminated. This procedure is continued until less than four loops are left and the receiver then fails. The noise value when this occurs is noted and compared against the corresponding noise value for the conventional receiver. The relative increase of interference noise for the VDLL receiver over the conventional receiver is then determined and shown in Table 2.

Table 2. Interference Improvements of a VDLL Receiver Over a Conventional GPS Receiver

Time (Hrs)	24 SV Constellation				An Actual Almanac Constellation		
	SVs in View	Improvement (dB)			SVs in View	Improvement (dB)	
		Equal Random Motion all 3 Axes	1/5 Less Severe Vertical Motion	No Vertical Motion		Equal Random Motion all 3 Axes	No Vertical Motion
0	9	3.3	3.8	4.2	11	4.3	5.5
1	10	3.5	4.3	4.8	12	4.8	6.1
2	6	2.1	3.3	3.4	12	5.0	6.0
3	8	3.5	4.0	4.2	12	5.0	6.4
4	6	2.0	2.6	3.1	10	4.1	6.1
5	7	2.7	2.8	2.9	7	2.7	4.6
6	8	3.1	4.2	4.5	10	4.1	5.8
7	7	2.9	3.3	3.6	11	5.2	6.1
8	7	2.2	3.6	3.8	11	5.0	6.2
9	8	2.6	3.6	4.0	12	5.1	6.2
10	8	3.2	3.7	4.1	10	4.1	5.4
11	7	2.9	3.4	3.9	9	3.9	5.2
12	8	3.1	3.6	4.0	11	4.4	5.5
13	9	3.8	4.6	4.6	12	4.8	6.1
14	7	2.8	3.2	3.5	12	5.0	6.0
15	9	4.2	4.2	4.4	12	5.0	6.4
16	7	2.6	2.9	3.3	10	4.1	6.2
17	6	1.6	2.7	2.9	8	3.7	4.6
18	7	3.3	3.8	4.1	10	4.2	5.9
19	8	3.2	4.1	4.6	11	5.2	6.0
20	8	2.9	2.9	3.1	11	5.0	6.2
21	8	2.9	3.7	4.0	12	5.1	6.2
22	7	2.7	3.3	3.6	10	4.1	5.4
23	8	3.1	3.5	4.2	9	3.9	5.2
Averages		**3.0**	**3.6**	**3.9**		**4.5**	**5.9**

To ensure that the difference in performance is not due to a poor tracking loop filter design in the conventional receiver, optimal Kalman filters are used for both the conventional receiver tracking loop filter and the VDLL receiver. The Kalman filters minimize the tracking loop errors for both the conventional receiver and for the VDLL receiver. We note the receiver filters, Kalman or otherwise, must have a bandwidth wide enough to track the user motion and the user clock but narrow enough to reject the noise. The filter design is thus determined, in part, by the models for user motion, the user clock, and interference noise. For the results generated in this paper, a second order user motion model and second order receiver clock model were used. The 1σ user motion for each axis for two motion models is shown in Figure 1. The less severe model with driving noise of q=125 m^2/sec^3 is used for the results shown in Table 2. The user clock model is also second order with 100 times better performance than the position error shown in Figure 1.

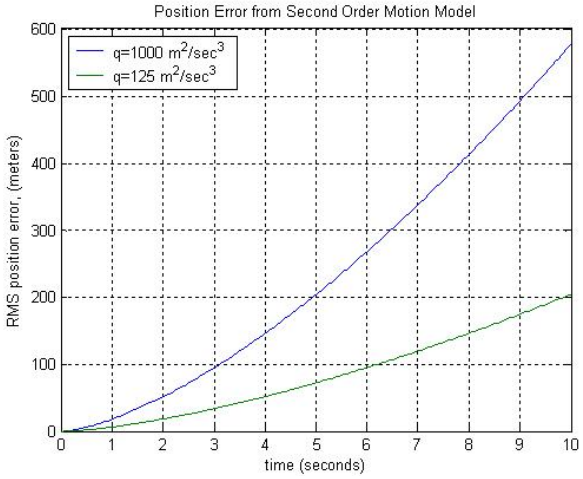

Figure 1. Position Errors from Second Order Random Motion Models

The second order position error model is doubly integrated white noise:

$$\ddot{\delta x} = w_{x1} \quad \text{Second order position motion model} \qquad (19)$$

Or in state space notation the model is:

$$\begin{bmatrix} \dot{\delta x} \\ \dot{\delta x}_1 \end{bmatrix} = \begin{bmatrix} 0 & 1 \\ 0 & 0 \end{bmatrix} \begin{bmatrix} \delta x \\ \delta x_1 \end{bmatrix} + \begin{bmatrix} 0 \\ w_{x1} \end{bmatrix} \quad \text{State space position motion model} \qquad (20)$$

The covariances are given by the linear variance equation:

$$\dot{P} = FP + PF^T + Q \quad \text{Linear variance equation} \qquad (21)$$

$$F = \begin{bmatrix} 0 & 1 \\ 0 & 0 \end{bmatrix}; \quad Q = \begin{bmatrix} 0 & 0 \\ 0 & q \end{bmatrix} \quad F \text{ and } Q \text{ matrices for motion model} \qquad (22)$$

and q takes on the values shown in Figure 1. Initial conditions on the P matrix can be neglected because we are evaluating the steady state tracking filter covariance which is independent of initial conditions.

The direction cosine matrices (DCM) for the αs from the user to the satellites were generated by Dr. L. F. Wiederholt with his MITRE GNSS Navigation Performance Evaluator [6]. The DCMs are selected every hour over 24 hours at the same latitude as Baghdad. Two constellations were used: a 24 SV generic GPS constellation and an actual GPS constellation for 11 April 2006 with 28 SVs in the constellation. The number of SVs in view and their DCMs were determined for elevations above 5 degrees.

The last remaining models that we need are the noise models, η_{TL} for the discriminator measurements in Equations (1) and (9). The variance of the noise for the i^{th} satellite for a one chip difference between the early and late sample is given in [4, pg 348] as:

$$RN_{di} = \frac{2N_0^2}{T_D^2} + \frac{P_i N_0}{T_D} \quad \text{Discriminator noise variance (watts}^2\text{)} \qquad (23)$$

P_i is signal power of the i^{th} satellite
T_D is coherent integration time
N_0 is wide band jamming noise density

With some additional rearranging of the terms, N_0/P_i is the independent variable rather than P_i and N_0 separately. For the results discussed in this paper, we use a coherent integration time of 1 millisecond. A short coherent integration time has the benefit of a less rapid decrease in signal power caused by clock drift and/or user velocity changes (see discussion associated with Equation (25)). Since an update time step of 1 millisecond for a Kalman filter would take significant computer time to determine the error covariances, the discrete noise given by Equation (23) is approximated by continuous noise, and the continuous form of the Kalman filter can be used with a much larger step size. The continuous approximation is given by:

$$RN_{ci} = RN_{di} T_D \quad \text{Continuous approximation} \qquad (24)$$

We now have all the procedures, equations, and values necessary to determine the interference performance improvement of a VDLL receiver over a conventional receiver. We also note the following assumptions: ionospheric and troposhperic errors and multipath errors are neglected, and the antenna gain is constant. We will discuss more on iono, tropo, and multipath later in a follow-on report. Antenna gain variations with elevation can make some difference in the results, but this is an additional complexity that clouds the basic understanding, and those results can be determined and also discussed in a follow-on report.

The covariance of the errors was determined by the procedures discussed above and the results are summarized in Table 2.

2.1 EFFECT OF DOPPLER ERRORS ON DISCRIMINATOR MEASUREMENTS

Even though we have lost carrier tracking, we must still down convert the GPS signals to baseband to obtain I&Q. If the receiver oscillator did not drift, the satellites did not move, and the user velocity did not change, we would continue to have exact carrier wipe-off as though there still was carrier tracking. However, because of unknown oscillator drift, satellite motion errors, and unknown user velocity changes from the time carrier tracking was lost, the frequency drift results in a power attenuation given by:

$$PL = \left(\frac{\sin \delta\omega T_D / 2}{\delta\omega T_D / 2} \right)^2 = \left(\frac{\sin \pi \delta f T_D}{\pi \delta f T_D} \right)^2 \qquad (25)$$

We have assumed that the clock drift and user/SV velocity is constant over each coherent integration time step, T_D, and δf is frequency drift due to receiver clock drift and velocity drift from the time of losing carrier tracking.

PL is the power attenuation due to frequency errors caused by receiver clock drift and user-to-SV range rate.

Equation (25) shows that a smaller coherent integration time allows for a larger frequency offset due to either receiver clock drift or due to SV-to-user velocity change. However, Equation (23) shows that a longer coherent integration time reduces the noise going into the filter. Thus there is a trade-off of signal power loss versus noise reduction as a function of coherent integration time.

The power attenuation is plotted in Figure 2 for a frequency error that could result from a receiver oscillator drift from the time carrier tracking was lost. Figure 3 shows the attenuation from user to SV velocity change from the time carrier tracking was lost. The velocity error from the time of losing carrier tracking was determined for the L_1 frequency where λ_1=0.19 m. Note that in Figure 3-3, 30 m/sec≅67 miles/hr. The effect of the attenuation would be a reduction in the power, P_i, in Equations (1) and (9).

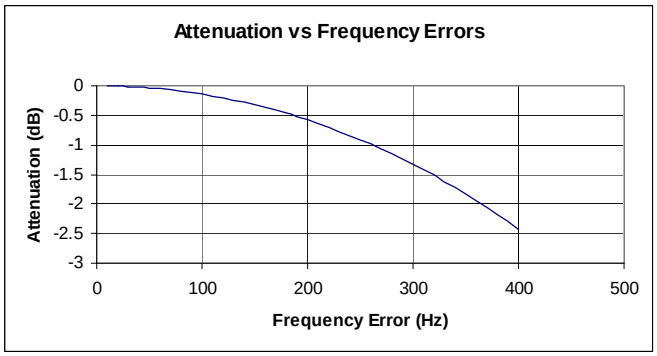

Figure 2. Power Attenuation Due to Receiver Clock Drift

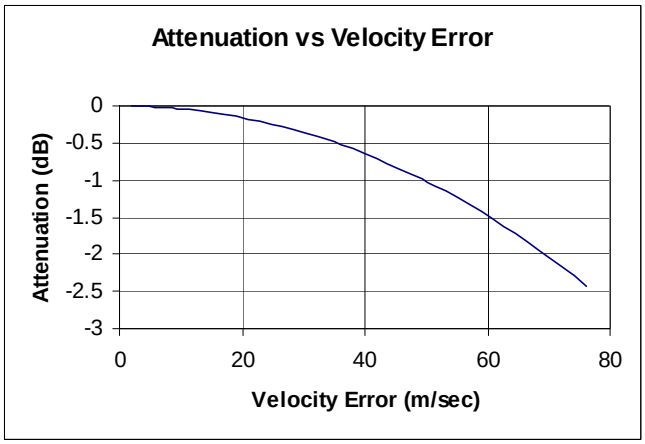

Figure 3. Power Attenuation Due to SV-to-User Velocity Change

We note that because of the motion models and clock models, the Kalman filter for the code tracking does perform some estimate of frequency drift.

3. IMBEDDING VDLL IN AN ULTRATIGHT OR DEEPLY INTEGRATED GPS RECEIVER

We will now describe how VDLL can be integrated with an ultratight or deeply integrated GPS receiver. In this way the interference benefits of a VDLL receiver can be realized when the inertial components degrade. To do this we must first describe the equations of an ultratight or deeply integrated GPS receiver and distinguish these equations from the VDLL equations. We will use the same assumptions that we have used in deriving the VDLL receiver, namely that the carrier loops have lost lock. In this case the equations greatly simplify. But first we make some simplifications in notation by combining Equations. (10-18) in more succinct form. Define:

$$\Delta p = \begin{bmatrix} \delta x_m \\ \delta y_m \\ \delta z_m \end{bmatrix} \tag{26}$$

$$\Delta T_{TL} = \begin{bmatrix} \Delta T_{TL1} \\ \vdots \\ \Delta T_{TLn} \end{bmatrix} \tag{27}$$

Now we can write the n pseudorange measurements as:

$$\Delta Z_{PR} = H_1 \Delta p + H_2 \Delta t_{Rm} + c\Delta T_{TL} \tag{28}$$

Where:

$$\Delta \dot{p} = F_p \Delta p + \eta_{\Delta p} \tag{29}$$

and H_1 and H_2 are determined from substitution.

We can write the n inertial system measurements along each of the user-to-SV directions as:

$$Z_{INS} = H_1 \Delta p + H_{2INS} \Delta p_{INS} \tag{30}$$

Where the INS errors are written in state space equation as:

$$\Delta\dot{p}_{INS} = F_{INS}\Delta p_{INS} + \eta_{INS} \qquad (31)$$

When inertial system measurements are subtracted from the GPS measurements, the true motion as defined here by Δp is eliminated. Thus, subtracting Equation (30) from Equation (28) we get the following n measurements:

$$\Delta Z_{PR} - Z_{INS} = -H_{2INS}\Delta p_{INS} + H_2\Delta t_{Rm} + c\Delta T_{TL}$$

n pseudorange minus n INS measurements (32)

Then the ultratight or deep integration equations are given by the n discriminator measurement equations, Equation (9), the n pseudorange minus INS measurement equations, Equation (32), and the receiver clock model Equations (17-18). Further discussion of UTC and DI GPS receivers are given in [7] and [8] and the references contained in them. If we embed the VDLL equations with the UTC or deep integration equations in addition to the INS error equations we also include the dynamics motion model. A summary of the equations for the three different GPS receiver configurations is given in Table 3, where again we remind the reader that these equations assume carrier tracking is lost.

If the equations for VDLL are compared with the equations for UTC or deep integration we see they are identical in form but the model of the dynamics motion model for VDLL is replaced with the model of the INS errors for UTC. If the INS performance in the UTC receiver degrades the receiver performance will not approach the VDLL performance because the dynamics motion is not modeled in UTC. However for the configuration shown in the last column in Table 3, when VDLL is embedded with UTC both the dynamics and the INS errors are modeled. In this case as the INS performance degrades the receiver performance will approach that of VDLL. If the INS degrades, the INS degradation has to be determined and included in the filter to properly weight the INS measurements. The means to effect this is not discussed in this paper. Generally, if the INS is performing normally, the INS errors have much lower variances and much narrower bandwidth than the dynamics motion. Thus the tracking filter bandwidth for UTC can be reduced substantially over that for VDLL.

Table 3. Summary of Interference and Accuracy Performance Equations for Three Different GPS Receiver Configurations

	VDLL	**UTC or Deep Integration**	**UTC or Deep Integration with Embedded VDLL**
Discriminator Measurements	$Z_{(EP-LP)1} = 2P_1\Delta T_{TL1} + \eta_{TL1}$ $\vdots$ $Z_{(EP-LP)n} = 2P_n\Delta T_{TLn} + \eta_{TLn}$	$Z_{(EP-LP)1} = 2P_1\Delta T_{TL1} + \eta_{TL1}$ $\vdots$ $Z_{(EP-LP)n} = 2P_n\Delta T_{TLn} + \eta_{TLn}$	$Z_{(EP-LP)1} = 2P_1\Delta T_{TL1} + \eta_{TL1}$ $\vdots$ $Z_{(EP-LP)n} = 2P_n\Delta T_{TLn} + \eta_{TLn}$
Pseudorange Measurements	$\Delta Z_{PR} = H_1\Delta p + H_2\Delta t_{Rm} + c\Delta T_{TL}$	$\Delta Z_{PR} - Z_{INS} = -H_{2INS}\Delta p_{INS} + H_2\Delta t_{Rm} + c\Delta T_{TL}$	$\Delta Z_{PR} = H_1\Delta p + H_2\Delta t_{Rm} + c\Delta T_{TL}$
INS Measurements	Not Applicable	INS measurements differenced with pseudorange measurements and shown in above entry	$Z_{INS} = H_1\Delta p + H_{2INS}\Delta p_{INS}$
Dynamics Motion Model	$\Delta\dot{p} = F_p\Delta p + \eta_{\Delta p}$	True dynamics motion cancels and is replaced by INS error model shown in entry below	$\Delta\dot{p} = F_p\Delta p + \eta_{\Delta p}$
INS Error Model	Not Applicable	$\Delta\dot{p}_{INS} = F_{INS}\Delta p_{INS} + \eta_{INS}$	$\Delta\dot{p}_{INS} = F_{INS}\Delta p_{INS} + \eta_{INS}$
Receiver Clock Model	$\Delta\dot{t}_{Rm} = F_C\Delta t_{Rm} + \eta_C$	$\Delta\dot{t}_{Rm} = F_C\Delta t_{Rm} + \eta_C$	$\Delta\dot{t}_{Rm} = F_C\Delta t_{Rm} + \eta_C$

4. CONCLUSIONS

- This paper has developed a methodology and corresponding equations for GPS interference and accuracy assessment that are easy to understand and use.
- Implementing a VDLL receiver can gain 3-6 dB in interference performance capability over a conventional GPS receiver.
- Additional benefits include: no additional hardware, no increase in power requirements, no increase in weight, and no decrease in reliability.

- A VDLL receiver can implement different filter bandwidths to accommodate differences that may be expected in vertical and horizontal motions. Because of this feature additional improvement to VDLL interference performance can be achieved by tailoring different horizontal and vertical bandwidths to expected specific user motions. For example, a hand-held user would be expected to have faster horizontal motions than vertical motions. A conventional receiver cannot do this.
- The form of the VDLL equations is the same as that for UTC or deep integration. In UTC or deep integration the error equations for the INS replace the error model of the dynamic motion used in VDLL.
- If the INS degrades in UTC or DI then the performance can approach that of VDLL if the model for dynamic motion is also included. A method to determine the degree of INS degradation also should be part of the mechanization to properly weight the INS measurements.

5. RECOMMENDATIONS

This paper has demonstrated the interference benefits of a VDLL GPS receiver based on a number of reasonable assumptions. Many of these assumptions remain to be quantitatively verified but should not stand in the way of a prototype receiver incorporating the additional features discussed in this paper and its filter design. The additional effort remaining to be accomplished has been identified in the body of this paper and these items as well as other items are summarized below.

1. Show that the carrier loops lose lock before the code loops.
2. Include the effects of iono, tropo, and multipath errors.
3. Determine the effect of antenna gain on performance.
4. Determine a loss-of-lock decision function for a VDLL receiver.
5. Determine methods to quantify the degree of INS degradation if VDLL is embedded with INS in a UTC or deep integration GPS receiver.
6. Perform a filter performance sensitivity analysis where the filter assumes certain design values, but the true values are different.

ACKNOWLEDGEMENTS

I would like to thank members of the Technical Staff at MITRE for reviewing the MITRE Technical Report that led to this paper, especially Dan Moulin and Ed Mitchell.

REFERENCES

1. Benson, D., 17 October 2002, *Benefit of High Power Satellite Using Vector Tracking*, Internal MITRE Memo.
2. Parkinson, B. W. and J. J. Spilker, editors, 1996, *Global Positioning System: Theory and Applications Volume 1*, Chapter 8, AIAA, ISBN 1-56347-106-X.
3. GRAM Specification (GPS-GRAM_001A, 25 February 1998).
4. Misra, P. and P. Enge, 2001, *Global Positioning System Signals, Measurements, and Performance*, Ganga-Jamuna Press, ISBN 0-9709544-0-9.
5. Kaplan, E. D. and C. J. Hegarty, editors, 2006, *Understanding GPS, Principles and Applications*, 2nd edition, Artech House, ISBN 1-58053-894-0.
6. Wiederholt, L. F., November 2005, User's Manual for the GNSS Navigation Performance Evaluator, MITRE WN 05B0000083.
7. Abbott, et al, *Global Positioning Systems and Inertial Measurement Unit Ultratight Coupling Method*, U.S. Patent 6,516,021, Feb 4, 2003.
8. Landis, D., et. al., *A Deep Integration Estimator for Urban Ground Navigation*, PLANS 2006.